Electronic Supplementary Material (ESI) for Nanoscale.

Wafer-Scale Single-Domain-Like Graphene by Defect-Selective Atomic Layer Deposition of Hexagonal ZnO

Kyung Sun Park[†], Sejoon Kim[†], Hongbum Kim[†], Deokhyeon Kwon[†], Yong-Eun Koo Lee[†], Sung-Wook Min[§], Seongil Im[§], Hyoung Joon Choi[§], Seulky Lim[‡], Hyunjung Shin[‡], Sang Man Koo[ǁ] and Myung Mo Sung[†]**

[†]Department of Chemistry, Hanyang University, Seoul 133-791, Korea

[§]Department of Physics and Applied Physics, Yonsei University, Seoul 120-749, Korea

[‡]Department of Energy Science, Sungkyunkwan University, Suwon 440-746, Korea

[ǁ]Department of Chemical Engineering, Hanyang University, Seoul 133-791, Korea

Corresponding Author: smm@hanyang.ac.kr, semicon@yonsei.ac.kr

Supporting Information

Dark-field optical microscopy (DF-OM). DF-OM (20× magnification, Olympus BX-51) was used to obtain images of the ZnO-stitched CVD graphene samples.

Scanning electron microscopy (SEM). A field-emission scanning electron microscope (FESEM, Hitachi S4800) was used to examine the surface morphology of CVD graphene with/without ZnO stitching and investigate the ZnO growth mode on the graphene grain boundaries by ALD. An accelerating voltage was 15 keV for imaging.

Transmission electron microscopy (TEM). CVD graphene is transferred to Au Quantifoil TEM grids (658-200-Au) using a direct transfer method.[S1] The carbon film side of the Quantifoil grid was placed onto CVD graphene/copper foils. Then isopropyl alcohol dropped on top of the grid and dried at 120 °C to allow the carbon film in the grid to come in contact with the CVD graphene film. The grid with graphene was dipped into 0.1 M ammonium persulphate aqueous solution to etch the underlying copper foil. The grid was finally rinsed with ethanol quite carefully and was annealed at 180 °C for 10 min to remove further residue or contaminants on the surface. The Quantifoil TEM grid with graphene was transferred to the ALD chamber to deposit ZnO with 30 ALD cycles. Dark-field (DF) TEM imaging was performed at 200 keV for grain boundary mapping (Supporting Information, Figure S4). High resolution (HR) TEM imaging was performed on a JEOL-ARM200F equipped with a monochromated beam giving a spatial resolution of better than 1 Å, which enables us to resolve individual carbon atoms at the grain boundaries (Supporting Information, Figure S5). HR TEM was operated at 80 keV to minimize the electron beam damage to the graphene samples (see Figure 1f and Supporting Information, Figure S7).

Atomic force microscopy (AFM). The topographic AFM and conductive AFM (C-AFM) analysis were performed simultaneously by using a SPA-400 (Seiko). NCHR silicon tips (Nanoworld) with a force constant of 42 Nm^{-1} and resonance frequency of 330 kHz were used in non-contact mode for topography imaging. Electrically conductive tips, PtIr5 coated Si probes (CONTPt, Nanoworld), were used in contact mode for the C-AFM analysis. The tips with a low force constant of 0.2 Nm^{-1} were grounded. The electrical contacts were patterned by e-beam lithography using JEOL JBX9300FS, following Cr/Au (5/35 nm) deposition on CVD graphene by an e-beam evaporator (ULTECH). Silver paste was used to achieve the contacts with the Cr/Au electrodes. A range of bias 0.05 to 1 V was applied between the tip and the electrode for local I-V (current-voltage) measurement. To avoid the mechanical contact instability, the load on the tip was kept constant as 0.3 nN in all the I-V measurements.

Electrical measurement. Sheet resistance of the graphene samples and current–voltage (I–V) properties of the graphene FETs were measured with a semiconductor parameter analyzer (HP 4155C, Agilent Technologies). The capacitance-voltage (C–V) measurements at 1 MHz were performed for our dielectric with an LCR meter (HP 4284, Agilent Technologies). All measurements were performed in dark at ambient air.

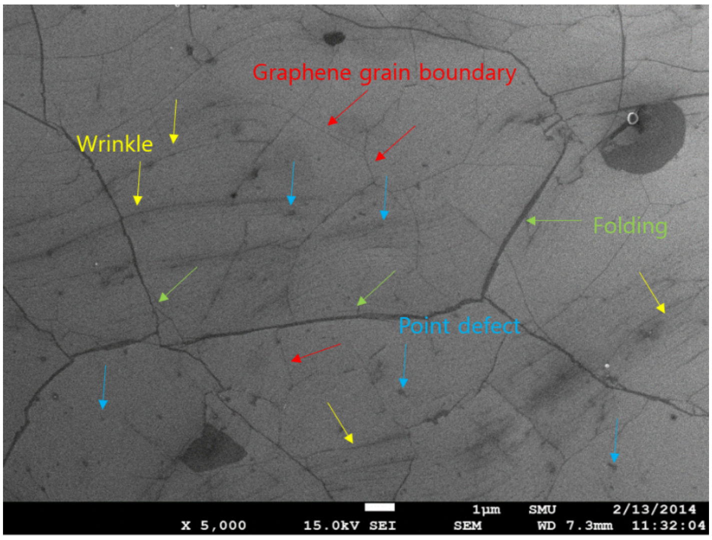

Figure S1. SEM image of CVD graphene film transferred onto a SiO_2/Si substrate. The image demonstrates that CVD graphene contains undesirable many defects. The colored arrows indicate the line defects such as grain boundaries (red), wrinkles (yellow) and foldings (green), and point defects (blue), respectively. The grain boundaries and point defects can be produced depending on substrates and processing conditions. The wrinkles on a graphene surface are formed due to the different thermal expansion coefficient between Cu and graphene during the process.[S2] A wet transfer of graphene onto a SiO_2/Si substrate also results in many line defects including ripples and foldings and so on.[S3]

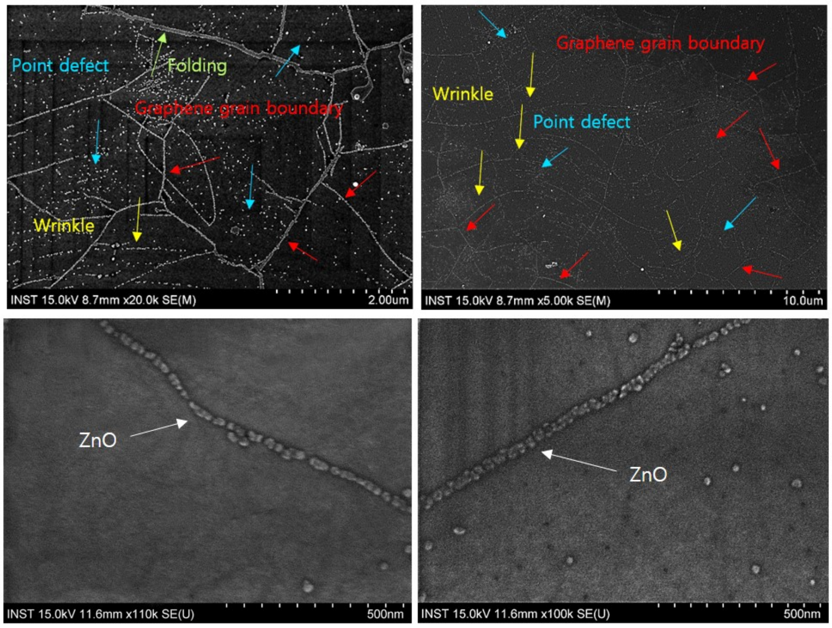

Figure S2. SEM images of the ZnO-stitched CVD graphene films. The colored arrows indicate the line defects such as grain boundaries (red), wrinkles (yellow) and foldings (green), and point defects (blue), respectively.

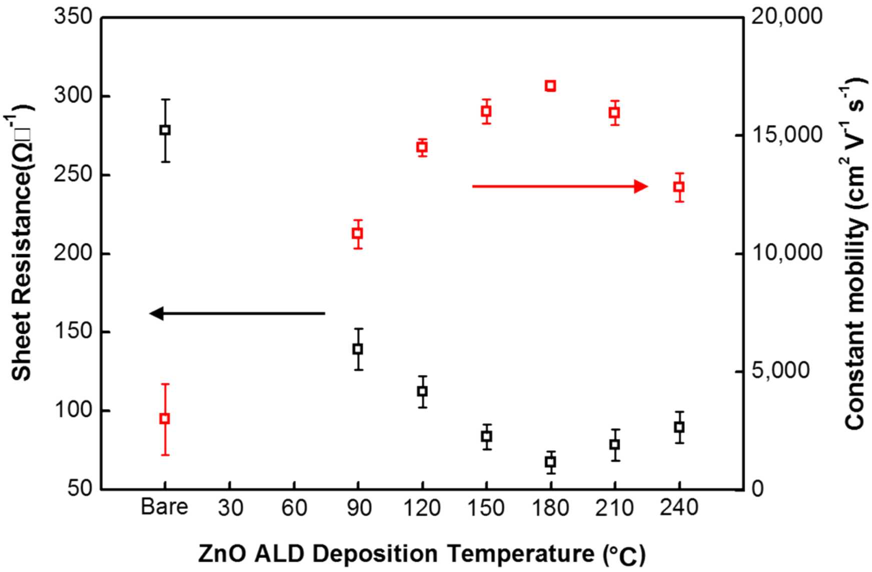

Figure S3. Sheet resistance and field effect mobility of the single layer bare CVD graphene and ZnO-stitched graphene films as a function of the deposition temperature of ALD. A 4-point probe measurements and FET characterizations were performed on SiO_2/p^+-Si substrate under ambient condition. Typical transfer characteristics (drain current versus gate voltage: I_{DS}-V_{TG} at V_{DS} = 1 V) of CVD graphene FETs with/without ZnO stitching were obtained and then the constant mobilities were derived by a previously reported model.[S4]

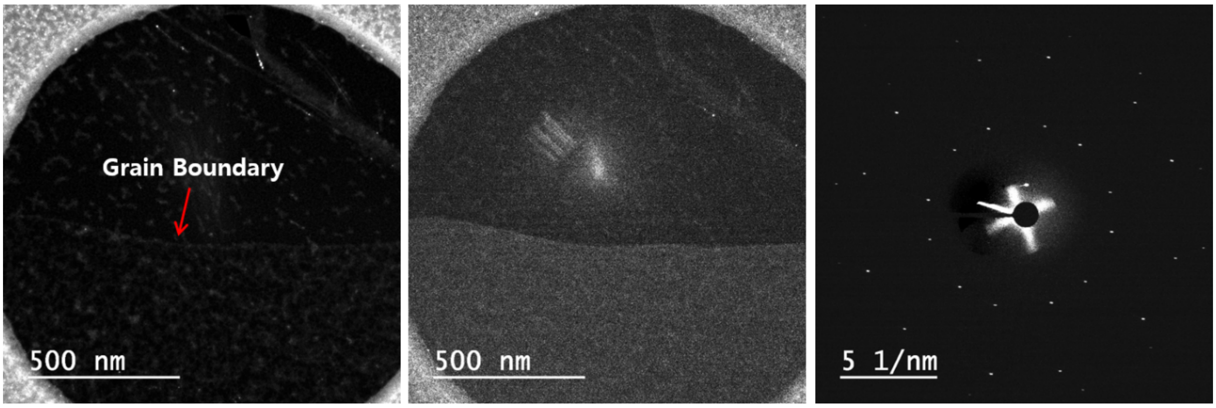

Figure S4. Low-magnification DF-TEM images of CVD graphene film after 30 ALD cycles of ZnO on the perforated carbon film. ZnO ALD visualizes many defects (white) including the grain boundary as indicated by a red arrow. The corresponding selective area electron diffraction (SAED) pattern shows two sets of the hexagonal pattern, indicating that the viewing region is composed of two grains merged with about 24° tilted angle.

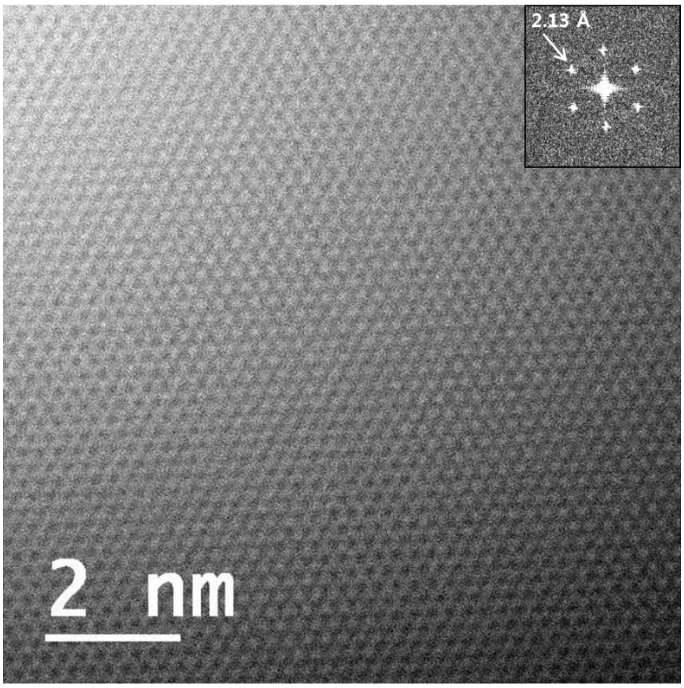

Figure S5. HR TEM image with Fast Fourier transform (FFT) (inset) of single-crystal monolayer CVD graphene. The atomic lattice structure of CVD graphene is shown to have a *d*-spacing of 2.13 Å.

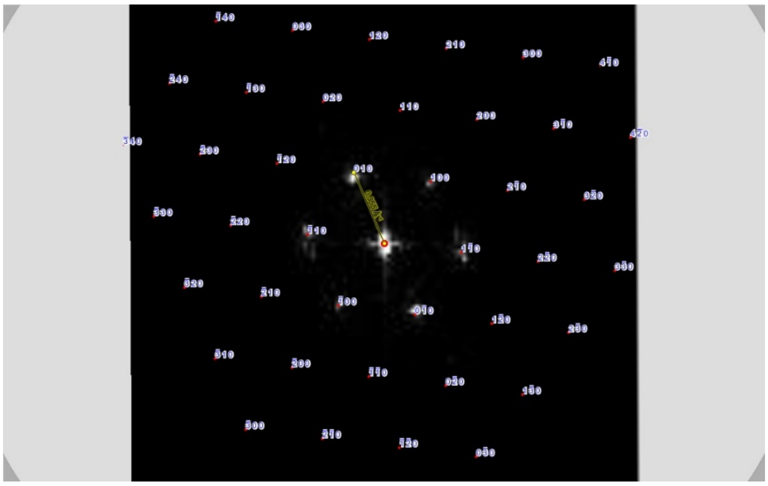

Figure S6. The FFT image from the region (iii) in Figure 1f along with the simulated diffraction pattern of (0001) wurtzite ZnO crystal by using Single Crystal 2.2.5. Crystal Maker Software Ltd..

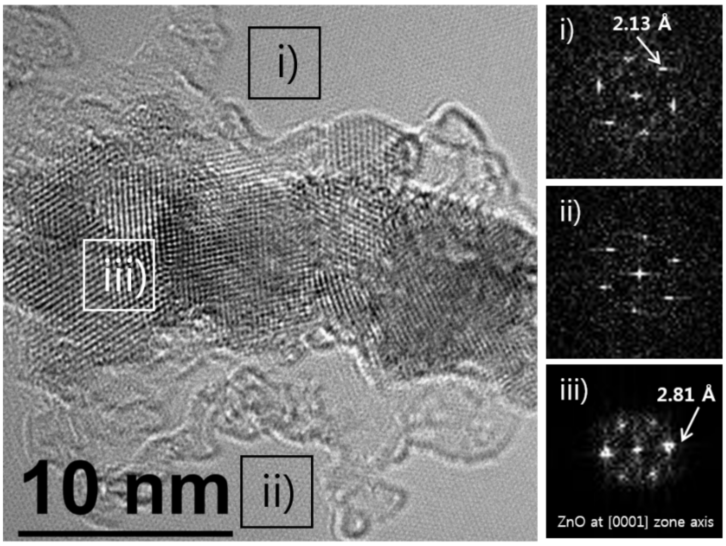

Figure S7. HR TEM image of representative chosen area from a sample shown in Figure S3, showing a grain boundary with ZnO stitching and its corresponding FFT images from selected areas denoted by i) - iii), respectively. The (i) and (ii) regions of the image are from different grains. The two grain orientations differ by 20°. The lattice distance of a graphene was obtained with d = 2.13 ± 0.05 Å. The FFT image of the region (iii) corresponds to wurtzite ZnO grown with [0001] direction, meaing that the cyrstal planes of the ZnO corresponds to the (0001) planes.[S5] The lattice distance of wurtzite ZnO was revealed with d-spacing of 2.81 Å.

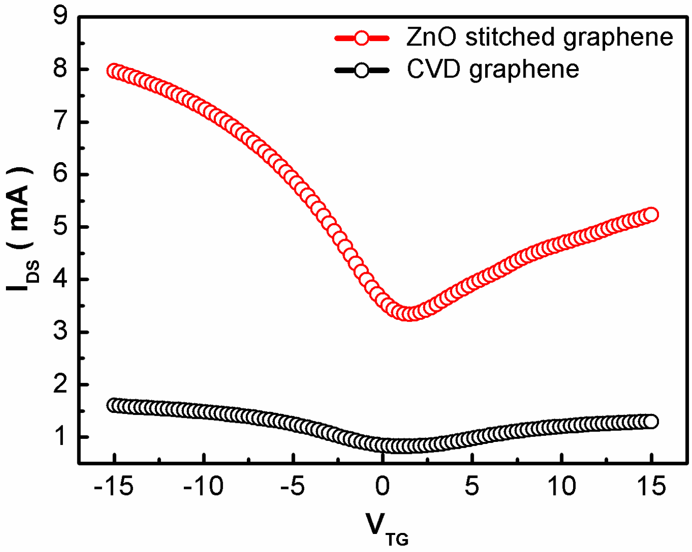

Figure S8. Representative I_{DS}-V_{TG} characteristic curves for the top-gated FETs with the bare CVD graphene and ZnO-stitched CVD graphene on a 4-inch SiO_2/p^+-Si wafer, respectively.

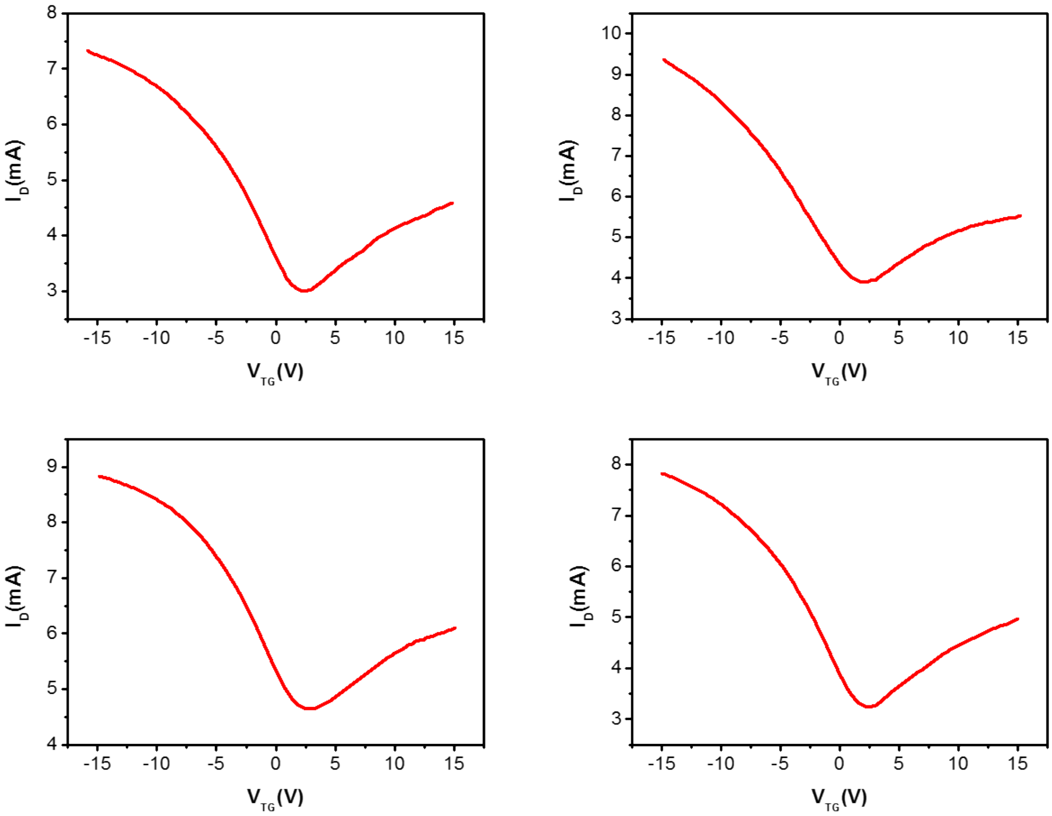

Figure S9. Typical transfer characteristics (drain current versus gate voltage: I_{DS}-V_{TG} at V_{DS} = 1 V) of CVD graphene FETs with ZnO ALD.

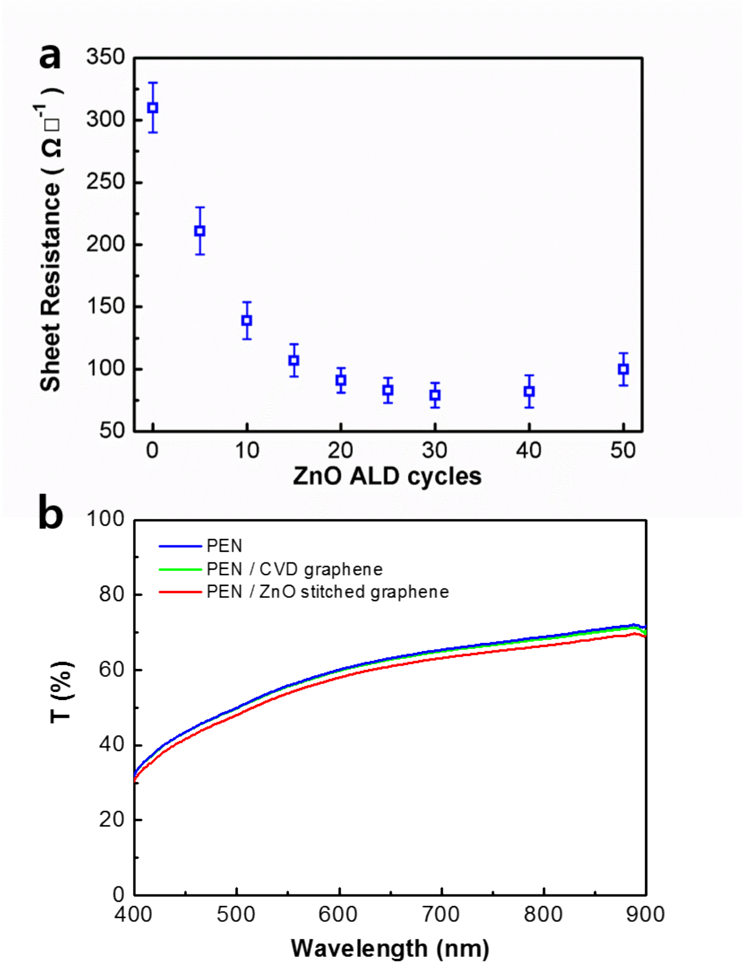

Figure S10. a, Sheet resistance (R_s) of the graphene films transferred on a PEN substrate as a function of the number of ZnO ALD cycles. **b,** Optical transmittance spectra of the bare PEN substrate, and bare and ZnO stitched CVD graphene on a PEN substrate.

References

(S1) Regan, W.; Alem, N.; Alemán, B.; Geng, B.; Girit, Ç.; Maserati, L.; Wang, F.; Crommie, M.; Zettl, A. *Appl Phys Lett* **2010**, *96*, 113102.

(S2) Li, X.; Cai, W.; An, J.; Kim, S.; Nah, J.; Yang, D.; Piner, R.; Velamakanni, A.; Jung, I.; Tutuc, E.; Banerjee, S. K.; Colombo, L.; Ruoff, R. S. *Science* **2009**, *324*, 1312-1314.

(S3) Li, X.; Zhu, Y.; Cai, W.; Borysiak, M.; Han, B.; Chen, D.; Piner, R. D.; Colombo, L.; Ruoff, R. S. *Nano Lett* **2009**, *9*, 4359-4363.

(S4) Kim, S.; Nah, J.; Jo, I.; Shahrjerdi, D.; Colombo, L.; Yao, Z.; Tutuc, E.; Banerjee, S. K. *Appl Phys Lett* **2009**, *94*, 062107.

(S5) Huang, X.; Willinger, M.; Fan, H.; Xie, Z.; Wang, L.; Klein-Hoffmann, A.; Girgsdies, F.; Lee, C.; Meng X. *Nanoscale* **2014**, 6, 8787-8795.